Journal of Power Sources 193 (2009) 804–809

Contents lists available at ScienceDirect

Journal of Power Sources

journal homepage: www.elsevier.com/locate/jpowsour

Effect of propane sultone on elevated temperature performance of anode and cathode materials in lithium-ion batteries

Mengqing Xu[a,b,c], Weishan Li[a,c,*], Brett L. Lucht[b,**]

[a] College of Materials Science and Engineering, South China University of Technology, Guangzhou 510641, China
[b] Department of Chemistry, University of Rhode Island, Kingston, RI 02881, United States
[c] Department of Chemistry, South China Normal University, Guangzhou 510006, China

ARTICLE INFO

Article history:
Received 16 January 2009
Received in revised form 5 March 2009
Accepted 31 March 2009
Available online 8 April 2009

Keywords:
Lithium-ion battery
Electrolyte
SEI
Propane sultone

ABSTRACT

A detailed investigation of the effect of the thermal stabilizing additive, propane sultone (PS), on the reactions of the electrolyte with the surface of the electrodes in lithium-ion cells has been conducted. Cells were constructed with meso-carbon micro-bead (MCMB) anode, $LiNi_{0.8}Co_{0.2}O_2$ cathode and 1.0 M $LiPF_6$ in 1:1:1 EC/DEC/DMC electrolyte with and without PS. After formation cycling, cells were stored at 75 °C for 15 days. Cells containing 2% PS had better capacity retention than cells without added PS after storage at 75 °C. The surfaces of the electrodes from cycled cells were analyzed via a combination of TGA, XPS and SEM. The addition of 2% PS results in the initial formation of S containing species on the anode consistent with the selective reduction of PS. However, modifications of the cathode surface in cells with added PS appear to be the source of capacity resilience after storage at 75 °C.

1. Introduction

Due to their high energy density, high discharge voltage, and long cycle life, lithium-ion batteries are a popular power source for advanced portable electronics [1]. A typical lithium-ion battery consists of a graphite anode, a transition metal oxide (such as $LiMn_2O_4$, $LiCoO_2$, $LiNiO_2$, etc.) cathode and a non-aqueous organic electrolyte, which acts as an ionic conductor between electrodes and separates the two materials. The electrolytes used in commercial lithium-ion batteries are prepared by dissolving $LiPF_6$ into binary or ternary solvents, which are typically mixtures of linear carbonates, including dimethyl carbonate (DMC), ethyl (-methyl-) carbonate (EMC) and diethyl carbonate (DEC), with ethylene carbonate (EC). However, commercial cells with $LiPF_6$-based electrolyte have several problems, including loss of power and capacity upon storage or prolonged use, especially at elevated temperature [2,3], which complicates the use of $LiPF_6$-based electrolytes in lithium-ion batteries for many large power applications, such as hybrid electric vehicles and satellites. Analyses of electrodes from lithium-ion cells that have undergone accelerated aging experiments suggest that electrolyte decomposition reactions result in the formation of surface films on both the anode and cathode [2,4–7]. The surface layers on both anode and cathode protect the electrodes from further reaction with the electrolyte, but they also create a barrier for lithium-ion intercalation/de-intercalation which increases cell impedance and decreases cycling efficiency. Degradation of the anode solid electrolyte interface (SEI) is one of the leading causes of capacity loss [2], and the impedance increases at the cathode are the major contributor to the cell impedance rise during cell aging [8]. Incorporation of low concentrations of additives into the electrolyte has been reported to improve interface layers, cycling stability, and high temperature performance of lithium-ion batteries.

Various electrolyte additives have been developed to assist the formation of a stable SEI on the graphite anode and improve the performance of lithium-ion batteries, such as vinylene carbonate (VC) [9,10], ethylene sulfite (ES) [11], 1,4-butane sultone (BS) [12], vinyl ethylene carbonate [13], and lithium bisoxalatoborate (LiBOB) [14]. These additives generally are more easily reduced than the electrolyte and produce an effective SEI layer. Although the beneficial effects of these additives on anodes are reasonably well understood, the effects on the cathode are rarely reported.

We have previously reported that 1,3-propane sultone (PS) can be used as an SEI forming additive on the anode to improve the cycling and high and low temperature discharge performance of lithium-ion batteries [15]. However, thorough understanding of the effect of PS addition on the anode SEI, thermal stability of the cell and surface reactions on the cathode are unclear. Herein, cyclic voltammetry, thermal gravimetric analysis (TGA), scanning electron microscopy with energy dispersive X-ray spectroscopy

* Corresponding author at: Department of Chemistry, South China Normal University, Guangzhou 510006, China. Tel.: +86 20 39310256; fax: +86 20 39310256.
** Corresponding author. Tel.: +1 401 874 5071; fax: +1 401 874 5072.
E-mail addresses: liwsh@scnu.edu.cn (W. Li), blucht@chm.uri.edu (B.L. Lucht).

0378-7753/$ – see front matter © 2009 Elsevier B.V. All rights reserved.
doi:10.1016/j.jpowsour.2009.03.067

(SEM-EDS), and X-ray photoelectron spectroscopy (XPS) are used to investigate the mechanism of PS reduction on anode surface along with the changes to the anode and cathode surfaces before and after thermal storage.

2. Experimental

Battery-grade carbonate solvents were obtained from EM industries without further purification. Battery-grade lithium hexafluorophosphate ($LiPF_6$) obtained from Hashimoto Chemical Corporation without further purification. Electrolyte solutions were prepared by dissolving 1 M $LiPF_6$ in the mixture carbonate solvents in a dry glove box ($H_2O < 1$ ppm) filled with high purity of argon. 1,3-propane sultone was purchased from Aldrich and dried over 4 Å molecule sieves before use. Most of the experiments were conducted with ternary electrolyte (1 M $LiPF_6$ EC:DEC:DMC (1:1:1, volume) with or without added 1,3-propoane sultone (PS) 2% (weight ratio).

A three-electrode cell was used for voltammetric measurements, with graphite as working electrode and Li foil as counter and reference electrodes. Electrochemical measurements were carried out on Autolab (PGSTAT30, ECO Echemie B.V. Company). Coin cells were fabricated in glove box filled with high purity argon with $LiNi_{0.8}Co_{0.2}O_2$ and MCMB as active materials and polypropylene as separator. The anode electrode contains 87% meso-carbon micro-bead (MCMB), 10% poly(vinylidene difluoride) (PVDF) binder and 3% conductive carbon dilutant; cathode electrode contains 89% $LiNi_{0.8}Co_{0.2}O_2$, 5% PVDF binder and 6% conductive carbon dilutant. Each coin cell contains 30.0 μL electrolyte. The coin cells were cycled at a constant current-constant voltage charge and a constant current discharge with 4.1 V and 3.0 V as cutoff voltages. The cells were cycled with the following procedure: first cycle at C/20, followed at C/10 and the remaining cycles at C/5. Samples were then stored at a full state of charge for 15 days at 75 °C. The cells were then cycled with both charge and discharge rates of C/5.

The anode and cathode electrodes were rinsed three times with DMC to remove $LiPF_6$ salt precipitated on the electrodes, and then evacuated overnight at room temperature before SEM, TGA and XPS analysis. The electrodes were exposed to air for less than 1 min, during the sample-introduction process, which does not change the surface morphology and composition. SEM and EDS analyses were conducted on a JEOL-5900 SEM. Thermal behaviors of the electrodes were analyzed on TA instruments SDT 2900 ramping the temperature from room temperature to 600 °C. The XPS spectra were conducted with a PHI 5500 system using Al Kα radiation ($h\upsilon = 1486.6$ eV) under ultra high vacuum. Lithium was not monitored due to its low inherent sensitivity and small change of binding energy. Calibration of XPS peak position was made by recording XPS spectra for reference compounds, which would be presented on the electrode surfaces: LiF, Li_2CO_3, $Li_xPO_yF_z$ and lithium alky-carbonate. The graphite peak at 284.3 eV was used as a reference for the final adjustment of the energy scale in the spectra. The spectra obtained were analyzed by Multipak 6.1A software and fitted using XPS peak software (version 4.1). A mixture of Lorentzian and Gaussian functions was used for the least-squares curves fitting procedure.

3. Results and discussion

3.1. Cyclic voltammery

Fig. 1 shows cyclic voltammograms of graphite electrodes in 1 M $LiPF_6$ EC:PC:EMC (1:1:3) with (b) and without (a) 1% PS. During the first cathodic potential sweep of electrolyte without PS, a reduction peak appears at around 0.5 V, which is attributed to the reduction of electrolyte, resulting in the formation of SEI

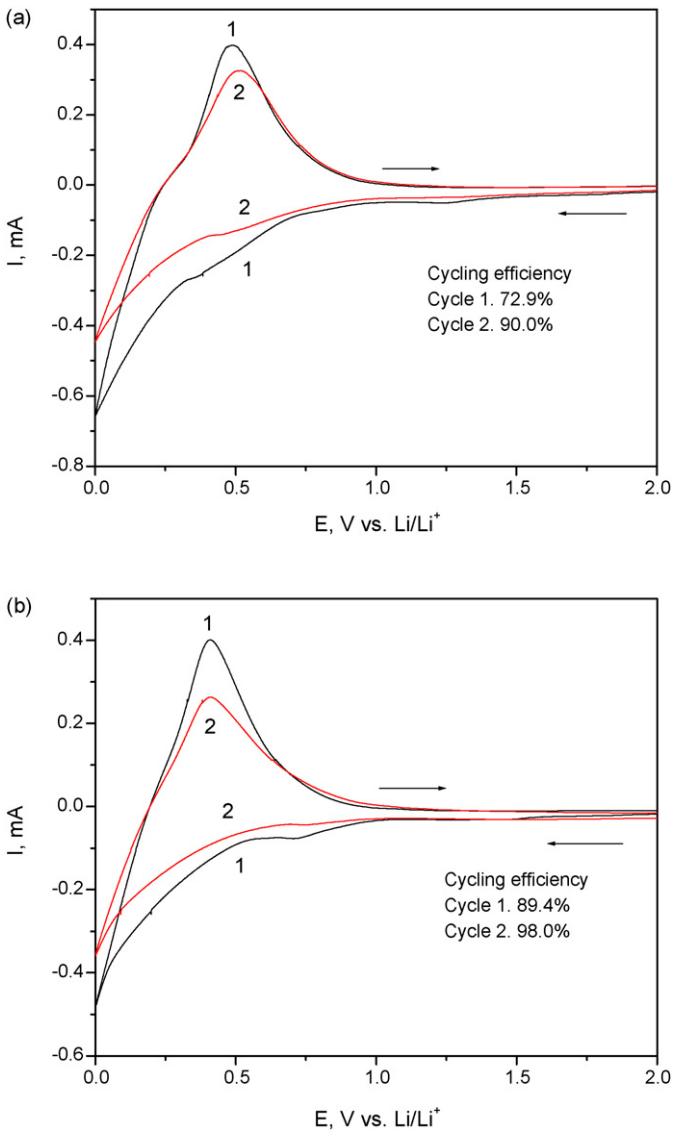

Fig. 1. Cyclic voltammograms of graphite electrodes in 1 mol L^{-1} $LiPF_6$/EC:PC:EMC (1:1:3) without (a) and with (b) 1 wt% PS, scan rate 0.5 mV s^{-1}.

film on graphite electrode. As the potential becomes more negative, the reduction current increases, which corresponds to an increase of quantity of lithium ions inserted into graphite. During the second sweep, the reduction peak at around 0.5 V can also be observed, but it is smaller than that of the first cycle. This indicates that the SEI film, formed on graphite electrode during the first cycle, does not completely suppress further reduction of electrolyte during the second cycle leading to additional irreversible capacity loss. A different behavior is observed in the presence of PS, Fig. 1b. During the first cathodic sweep, a reduction peak at around 0.7 V is observed. The new reduction peak is attributed to the reduction of PS on the graphite electrode and forming of the SEI film. With decreasing potential, the cathodic current slowly increases but there is no observable reduction peak at 0.5 V suggesting that the SEI film formed from PS effectively suppresses further electrolyte reduction on the graphite electrode. During the second sweep, the reduction peak at around 0.7 V is not observed, which is consistent with the formation of a stable PS derived anode SEI during the first cycle. The coulombic efficiency for the graphite electrode in the electrolyte without PS was estimated to be 72.9% and 90.0% for the first cycle and second cycle, respec-

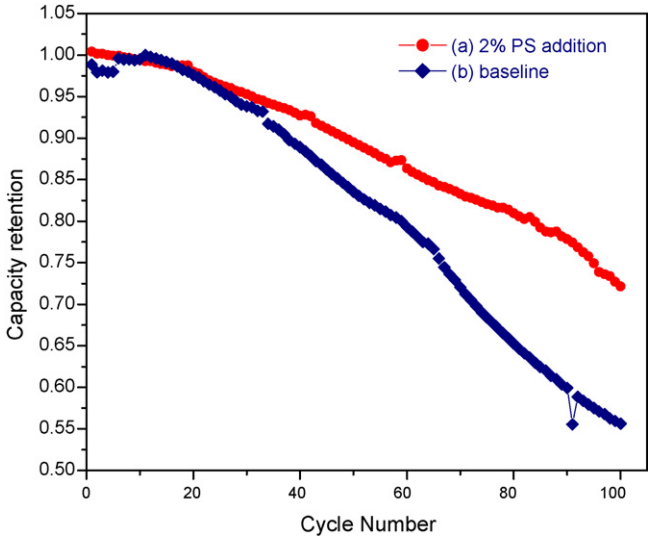

Fig. 2. Cycling performance of lithium-ion batteries after storage at 75 °C for 15 days (a) 1 M $LiPF_6$ EC:DEC:DMC (1:1:1) + 2% PS and (b) 1 M $LiPF_6$ EC:DEC:DMC (1:1:1).

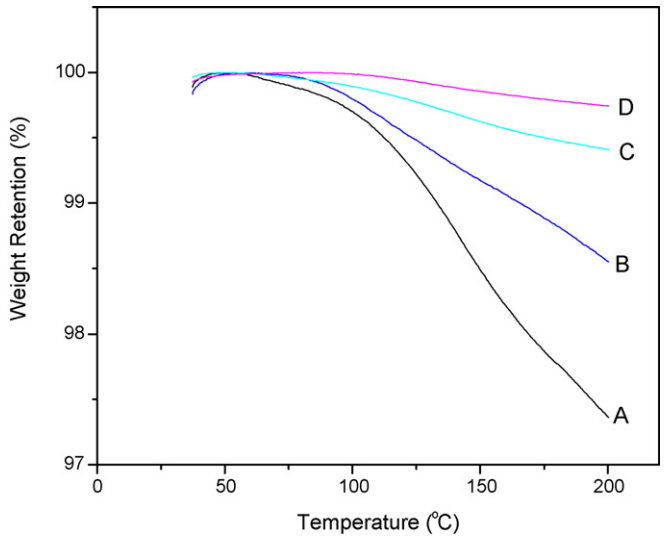

Fig. 3. Thermal gravimetric analysis for the samples: (A) anode electrode after storage at 75 °C for 15 days with PS; (B) cathode electrode after storage at 75 °C for 15 days with PS; (C) anode electrode after storage at 75 °C for 15 days without PS; (D) cathode electrode after storage at 75 °C for 15 days without PS.

tively. For the electrolyte with PS addition, the coulombic efficiency was estimated to be 89.4% and 98.0% for the first cycle and second cycle, respectively. The increase of coulombic efficiency can be ascribed to the PS participation in SEI formation on graphite electrode.

3.2. Cycling performance of lithium-ion batteries after thermal storage

Lithium-ion coin cells were constructed containing ternary electrolyte with and without 2% PS addition. After initial formation cycling the cells were stored at 75 °C for 15 days. Cell without PS retained only 56% of their initial reversible capacity after the storage period while cells with added PS retained 70% of their initial storage capacity. Continued cycling of the cells after storage at 75 °C for 15 days is depicted in Fig. 2. The normalized capacity retention after thermal storage is improved significantly via incorporation of PS. The capacity retention during the first 100 charge/discharge cycles after thermal storage is much higher for the cell containing PS (72%) than the cell without PS (56%). Surface analysis of electrodes extracted from cells with and without PS, as described below, provides insight into the source of the difference in capacity retention.

3.3. Thermal gravimetric analysis

The presence of organic species on the surface of anodes and cathodes was investigated with thermal gravimetric analysis (TGA) [16,17]. Fig. 3 shows the thermally induced weight loss of anode and cathode electrodes that were stored at 75 °C for 15 days with and without PS. The total weight losses are 2.6%, 1.4%, 0.6% and 0.3%, respectively. There are two clear trends in weight loss. First, addition of PS results in an increase in the weight loss for both the anode and cathode. This can be assigned to the decomposition of organic PS reduction products. Second, anodes have more weight loss than cathode electrodes, suggesting that the anode SEI is thicker and contains higher concentrations of organic components.

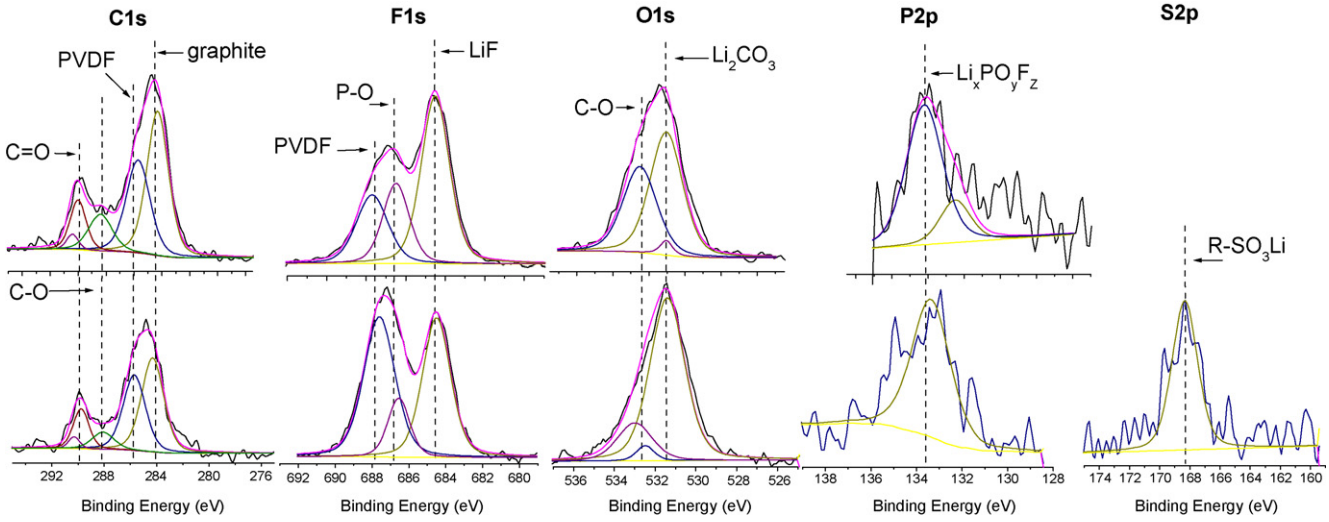

Fig. 4. C 1s, F 1s, O 1s, P 2p and S 2p XPS spectra of MCMB anode cycled in 1 M $LiPF_6$ EC:DEC:DMC (1:1:1, volume) (top) and in 1 M $LiPF_6$ EC:DEC:DMC (1:1:1, volume) + 2% PS (weight ratio) (bottom).

Table 1
Surface concentration of different elements on fresh anode and anodes from pre-cycled cells and after thermal storage cells with baseline ternary electrolyte and addition of 2% PS.

Sample	C 1s (%)	O 1s (%)	F 1s (%)	P 2p (%)	S 2p (%)
Fresh	67.1	3.8	29.1		
Cycled with ternary electrolyte	34.0	14.6	50.0	1.4	
Cycled with ternary electrolyte +2% PS	39.0	23.5	34.2	0.7	2.6
Cycled and stored at 75 °C	27.9	35.1	30.0	7.0	
Cycled and stored at 75 °C + 2% PS	24.4	37.7	29.0	8.2	0.7

3.4. Scanning electron microscopy of anodes

The surface of MCMB particles from cycled electrodes containing electrolyte with and without PS before and after storage at 75 °C for 15 days was further investigated with scanning electron microscopy (SEM). The surface of the graphite particles is very similar, suggesting that the presence of PS does not result in significant modification to the bulk MCMB particles. The graphite particles still have a similar appearance after storage at 75 °C for 15 days in the electrolytes with and without PS addition, suggesting the thermal storage does not modify the bulk structure of the MCMB particles with or without added PS.

3.5. XPS analysis of MCMB anode electrodes

The surface composition in the SEI layer of the anode cycled in 1 M $LiPF_6$ EC:DEC:DMC (1:1:1) and in 1 M $LiPF_6$ EC:DEC:DMC (1:1:1) + 2% PS (wt%) was investigated by X-ray photoelectron spectroscopy (Fig. 4). The cell cycled with ternary baseline electrolyte results in a decrease in the concentration of C and an increase in the concentration of F, O, and P (Table 1) compared to the fresh uncycled anode. This is consistent with the formation of an anode SEI covering the MCMB graphite and PVDF binder. Analysis of the C 1s spectrum reveals that the intensity of the peak located at 284.3 eV, assigned to graphite, and the peaks located at 285.7 eV and 290.4 eV, corresponding to PVDF binder, are diminished compared to the fresh anode as expected from the formation of the anode SEI. The surface of MCMB anode contains many species characteristic of electrolyte decomposition products. New peaks are observed in the 287.5–290 eV range suggesting the presence of Li_2CO_3 (290 eV), lithium alkyl carbonates (R–CH_2OCO_2Li, 287.5 eV and R–CH_2OCO_2Li, 288.5 eV), alkanes (285 eV) and ethers (286 eV) [6,18]. The major peaks in O 1s spectra at 531.6 eV and 532.5–533.5 eV correspond to Li_2CO_3 and lithium alkyl carbonates (R–CH_2O(C=O)OLi (532.5 eV) and R–CH_2O(C=O)OLi (533.5 eV), respectively [6]. Analysis of the F 1s spectrum suggests three main peaks consistent with the presence of LiF (684.5 eV), and PVDF (687.6 eV). Examination of P 2p spectrum supports the presence of low concentrations of $Li_xPO_yF_z$ (134.5 eV) [5] and residual $LiPF_6$ (136.2 eV) [4].

Analysis of an MCMB composite anode extracted from a cell containing 2% PS addition suggests changes in surface compositions compared to anodes without PS: the C and O concentrations increase, while F concentration decreases, and S is present (Table 1). This indicates that the presence of PS modifies the anode SEI forming reactions. The peak at 168.5 eV in the S 2p spectrum confirms that PS participates in formation of the SEI film on the MCMB anode. This peak can be assigned to R–SO_3Li moieties, related to sodium benzensulfonate (168 eV, S 2p).

The surface composition of an MCMB composite anode extracted from a cell cycled with the baseline ternary electrolyte then stored at 75 °C for 15 days was investigated by XPS (Fig. 5, top). The surface composition is modified significantly upon thermal storage, the concentration of C is decreased while the concentrations of P and O are increased, consistent with a greater concentration of decomposition products of $LiPF_6$. Analysis of the C 1s spectrum suggests that there is a relative decrease in the concentration of Li_2CO_3 (290 eV) and increase in the concentrations of alkyl carbonates (287–288.5 eV) and ethers including polyethylene oxide (286 eV) [19]. The F 1s spectrum reveals a relative decrease in the concentration of LiF (684.5 eV) and increase in the concentration of $Li_xPO_yF_z$ (686.5–688 eV), which is consistent with the significant increase in the concentration of P. Analysis of P 2p spectrum supports the presence of $Li_xPO_yF_z$ (134.5 eV) while the O 1s spectrum contains a broad peak centered at ~532 eV consistent with a mixture of alkyl carbonates, ethers, and $Li_xPO_yF_z$.

The MCMB anode extracted from the cell containing ternary electrolyte with 2% PS addition after storage at 75 °C was investigated by XPS (Fig. 5, bottom) providing very similar results to the sample without PS. The decrease in S concentration, similarity of the elemental concentrations, and similarity of individual element spectra, suggest that the anode surface modifications that were present after initial cycling with PS are lost upon storage at 75 °C for 15 days.

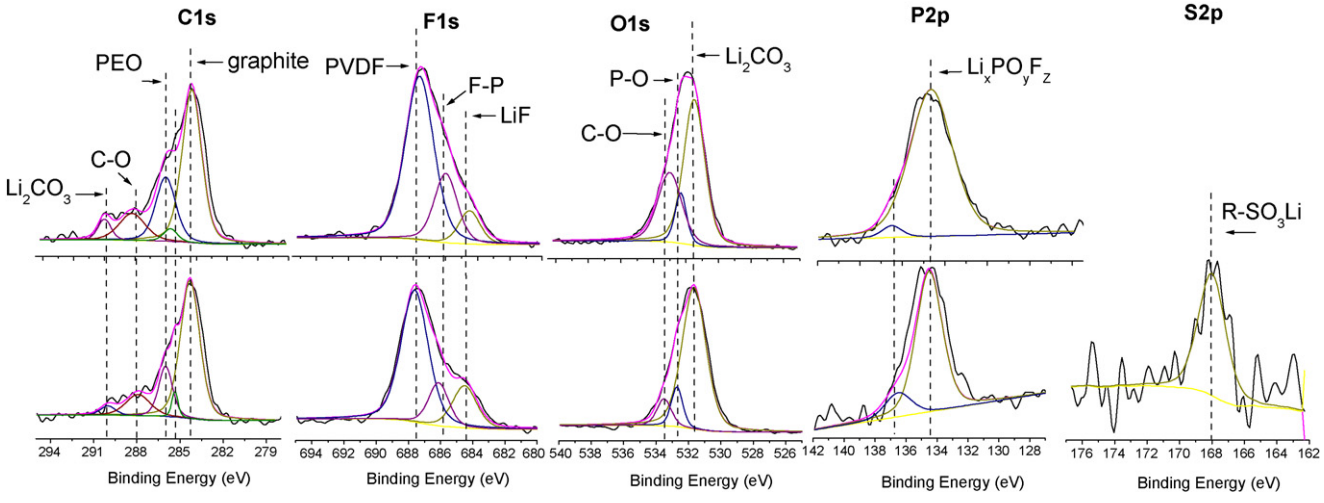

Fig. 5. C 1s, F 1s, O 1s, P 2p and S 2p XPS spectra of MCMB anode after storage at elevated temperature with the electrolyte 1 M $LiPF_6$ EC:DEC:DMC (1:1:1, volume) (top) and in 1 M $LiPF_6$ EC:DEC:DMC (1:1:1, volume) + 2% PS (weight ratio) (bottom).

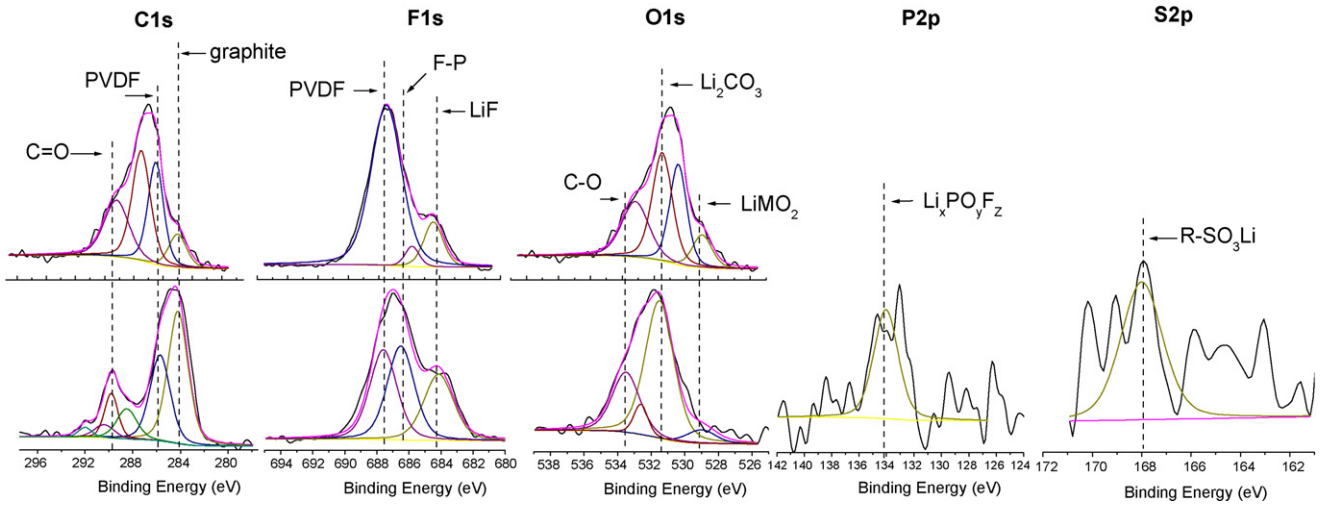

Fig. 6. C 1s, F 1s and O 1s XPS spectra of $LiNi_{0.8}Co_{0.2}O_2$ cathode precycled in 1 M $LiPF_6$ EC:DEC:DMC (1:1:1, volume) (top) and in 1 M $LiPF_6$ EC:DEC:DMC (1:1:1, volume) + 2% PS (weight ratio) (bottom).

3.6. SEM analysis of $LiNi_{0.8}Co_{0.2}O_2$

The $LiNi_{0.8}Co_{0.2}O_2$ particles from cycled electrodes and cycled electrodes stored at 75 °C for 15 days with and without PS addition were investigated with scanning electron microscopy. The bulk particles do not appear to be significantly effected by the presence or absence of PS in the electrolyte or storage at elevated temperature.

3.7. XPS analysis of $LiNi_{0.8}Co_{0.2}$ particles

XPS spectra from fresh $LiNi_{0.8}Co_{0.2}O_2$ cathode electrode have been previously reported [6]. The fresh electrode is characterized by peaks corresponding to PVDF binder at 687.6 eV in F 1s and 285.7 eV and 290.4 eV in C 1s. The peaks located at 284.3 in the C 1s spectrum are characteristic of graphite, and 290 eV is characteristic of the surface Li_2CO_3 which also contains a O 1s peak at 531.6 eV [4,20–22]. The peak at 684.5 eV is assigned to LiF, which is believed to come from the electrode preparation process [4]. The oxygen from the bulk metal oxide has a weak signal at 529 eV in the O 1s spectrum, due to the presence of the surface Li_2CO_3.

The surface of cathode particles cycled with ternary electrolyte with and without 2% PS was investigated by XPS. It can be seen that additional peaks appear in the spectra of $LiNi_{0.8}Co_{0.2}O_2$ samples after cycling (Fig. 6). The C 1s, F 1s and O 1s spectra of cycled samples in the electrolyte with and without PS addition are very similar. In addition to the peaks associated with PVDF, graphite, and Li_2CO_3, new broad peaks are observed in the C 1s spectra between 288 eV and 291 eV, consistent with C—O bonds, in lithium alkoxides (ROLi), esters or lithium alkyl carbonates [6]. The major peaks in O 1s spectra at 529 eV, 531.6 eV and 534 eV correspond to the bulk metal oxide, Li_2CO_3 and lithium alkyl carbonates, respectively, confirming that the surface films are still relatively thin. The F 1s spectra contain two main peaks: one at 684.5 eV assigned to LiF,

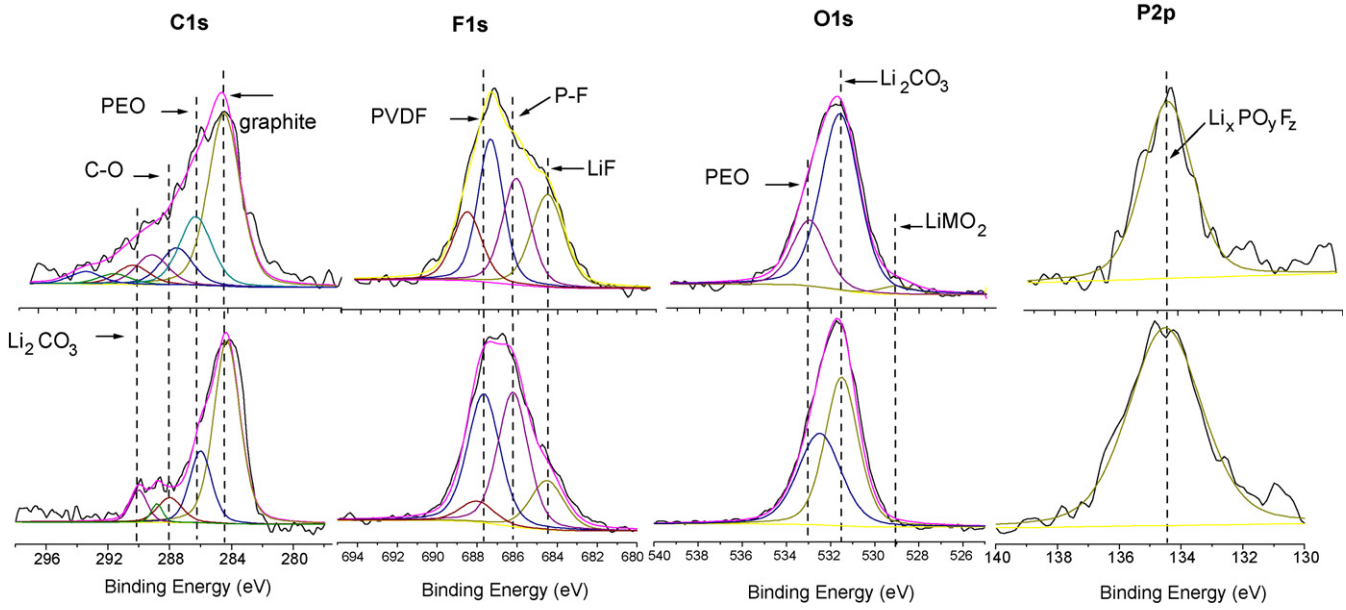

Fig. 7. C 1s, F 1s, O 1s and P 2p XPS spectra of $LiNi_{0.8}Co_{0.2}O_2$ cathode after thermal storaged with the electrolyte 1 M $LiPF_6$ EC:DEC:DMC (1:1:1, volume) (top) and in 1 M $LiPF_6$ EC:DEC:DMC (1:1:1, volume) + 2% PS (weight ratio) (bottom).

Table 2
Surface concentration of different elements on fresh cathode and cathodes from thermal storage cells with baseline ternary electrolyte and addition of 2% PS.

Sample	C 1s (%)	O 1s (%)	F 1s (%)	P 2p (%)	S 2p (%)
Fresh	55.9	10.1	30.0		
Cycled with ternary electrolyte	50.3	12.3	37.4		
Cycled with ternary electrolyte +2% PS	49.7	10.9	34.7	0.9	0.8
Cycled and stored at 75 °C	21.1	34.3	31.2	12.2	
Cycled and stored at 75 °C + 2% PS	34.3	33.1	29.6	4.9	

and another peak at higher binding energy (687.6 eV) assigned to PVDF.

Spectral analysis of $LiNi_{0.8}Co_{0.2}O_2$ cathodes cycled with ternary electrolyte and stored at 75 °C for 15 days suggests changes in surface composition (Fig. 7). The concentrations of C and F decrease, while the concentrations of O and P increase (Table 2). The increases in the concentration of O and P are consistent with generation of thicker films of electrolyte decomposition products on the surface of metal oxide. Analysis of C 1s spectrum reveals peaks at 286.7 eV can be assigned to polycarbonate, presumably from the polymerization of EC. Peaks in the 288–291 eV range suggest the presence of species containing C—O bonds, such as esters or lithium alkoxides, and lithium alkyl carbonates, R–CH_2OCO_2Li (288 eV) and R–CH_2OCO_2Li (289) eV. The concentration of Li_2CO_3 (290 eV) is decreased as previously reported for thermally abused cells [6]. The O 1s spectrum contains new signals at 532.5 eV, characteristic of polymeric species (polycarbonates or polyethylene oxide (PEO)). The metal oxide O 1s signal at 529 eV disappears, suggesting that the surface films are thicker than the escape depth of the photoelectrons. Examination of F 1s and P 2p spectra supports the presence of $Li_xPO_yF_z$ (687 eV, F 1s and 134.5 eV, P 2p). Enhancement of the F 1s signal at 684.5 eV supports an increase in the concentration of LiF after thermal storage.

Addition of PS to ternary electrolyte modifies the changes to the surface composition of the $LiNi_{0.8}Co_{0.2}O_2$ cathode after thermal storage. The cathode extracted from a cell containing 2% PS shows lower concentration of O, F, P and higher concentration of C (Table 2), which indicates that addition of PS modifies the structure of the cathode surface decreasing the concentration of inorganic components ($Li_xPF_yO_z$ and LiF) while increasing the concentration of organic species. This is consistent with the modified weight loss observed by TGA, as described above.

4. Conclusion

A detailed investigation of the effect of the thermal stabilizing additive, propane sultone, on the reactions of the electrolyte with the surface of the electrodes in lithium-ion cells has been conducted. Upon initial cycling, cells containing PS provide evidence for selective reduction of PS and the formation of anode SEIs containing PS. Storage of cells at 75 °C for 15 days results in a decrease in storage capacity for cells with and without PS. However, upon cycling cells containing PS have much better capacity retention. Analysis of the surfaces of the electrodes after storage at 75 °C and 100 cycles suggests that the improved performance of cells containing PS is due to modifications of the cathode surface films and not the anode SEI.

Acknowledgements

M. Xu thanks the financial support from the China Scholarship Council (CSC). B. Lucht thanks the URI Foundation Prototype Development Fund for financial support. W.S. Li thanks the financial support financial support from National Natural Science Foundation of China (NNSFC, 20873046) and Specialized Research Fund for the Doctoral Program of Higher Education (Grant No. 200805740004).

References

[1] K. Xu, Chem. Rev. 104 (2004) 4303.
[2] A.M. Andersson, K. Edstrom, J. Electrochem. Soc. 148 (2001) A1100.
[3] M.C. Wu, P.J. Chiang, J.C. Liu, J. Electrochem. Soc. 152 (2005) A1041.
[4] A.M. Andersson, D.P. Abraham, R. Hassch, S. MacLaren, J. Liu, K. Amine, J. Electrochem. Soc. 149 (2002) A1358.
[5] F.T. Quinlan, K. Sano, T. Willey, R. Vidu, K. Tasaki, P. Stroeve, Chem. Mater. 13 (2001) 4208.
[6] W. Li, A. Xiao, B.L. Lucht, M.C. Smart, B.V. Ratnakumar, J. Electrochem. Soc. 155 (2008) A648.
[7] D.S. Lu, W.S. Li, X.X. Zuo, Z.Z. Yuan, Q.M. Huang, J. Phys. Chem. C 111 (2007) 12067.
[8] J.P. Christophersen, C.D. Ho, C.G. Motloch, D. Howell, H.L. Hess, J. Electrochem. Soc. 153 (2006) A1406.
[9] D. Aurbach, K. Gamolsky, B. Markovsky, Y. Gofer, M. Schmidt, U. Heider, Electrochim. Acta 47 (2002) 1423.
[10] T. Sasaki, T. Abe, Y. Iriyama, M. Inaba, Z. Ogumi, J. Electrochem. Soc. 152 (2005) A2046.
[11] M. Lu, H. Cheng, Y. Yang, Electrochim. Acta 53 (2008) 3539.
[12] M.Q. Xu, W.S. Li, X.X. Zuo, J.S. Liu, X. Xu, J. Power Sources 174 (2007) 705.
[13] J. Li, W.H. Yao, Y.S. Meng, Y. Yang, J. Phys. Chem. C 112 (2008) 12550.
[14] K. Xu, U. Lee, S. Zhang, M. Wood, T.R. Jow, Electrochem. Solid-State Lett. 6 (2003) A144.
[15] X.X. Zuo, M.Q. Xu, W.S. Li, D.G. Su, J.S. Liu, Electrochem. Solid-State Lett. 9 (2006) A196.
[16] E.P. Roth, D.H. Doughty, J. Franklin, J. Power Sources 134 (2004) 222.
[17] A.D. Pasquier, F. Disma, T. Bowmer, A.S. Gozdz, G. Amatucci, J.-M. Taracon, J. Electrochem. Soc. 145 (1998) 472.
[18] A. Schechter, D. Aurbach, H. Cohen, Langmuir 15 (1999) 3334.
[19] M.N. Richard, J.R. Dahn, J. Electrochem. Soc. 146 (1999) 2068.
[20] D. Aurbach, B. Markovsky, I. Weissman, E. Levi, Y. Ein-Eli, Electrochim. Acta 45 (1999) 67.
[21] T. Eriksson, A.M. Andersson, A.G. Bishop, C. Gejke, T. Gustafsson, J.O. Thomas, J. Electrochem. Soc. 149 (2002) A69.
[22] D. Ostrovskii, F. Ronci, B. Scrosati, P. Jacobsson, J. Power Sources 94 (2001) 183.